# On the Formation of Radial Tidal Current off the Central Jiangsu Coast

Peng Yao
*PhD student, Faculty of Civil Engineering and Geosciences, Delft University of Technology, Delft, 2600 GA, The Netherlands; College of Harbour, Coastal and Offshore Engineering, Hohai University, Nanjing 210098, China. Email: P.Yao@tudelft.nl*

M.J.F. Stive
*Professor, Faculty of Civil Engineering and Geosciences, Delft University of Technology, Delft, 2600 GA, The Netherlands.. Email: M.J.F.Stive@tudelft.nl*

Changkuan Zhang
*Professor, College of Harbour, Coastal and Offshore Engineering, Hohai University, Nanjing 210098, China. E-mail: ckzhang@hhu.edu.cn*

Min Su
*PhD student, Faculty of Civil Engineering and Geosciences, Delft University of Technology, Delft, 2600 GA, The Netherlands; College of Harbour, Coastal and Offshore Engineering, Hohai University, Nanjing 210098, China. Email: M.Su@tudelft.nl*

Zhengbing Wang
*Professor, Faculty of Civil Engineering and Geosciences, Delft University of Technology, Delft, 2600 GA The Netherlands; Deltares, Delft, 2600 MH, The Netherlands. E-mail: Zheng.Wang@deltares.nl*

**ABSTRACT:** In the South Yellow Sea off the Jiangsu coast, there exists a special type of sand bodies, which are known as radial sand ridge field (RSRF). One of the characteristics of this area is the distinctive radial tidal current field. Although many studies have focused on the hydrodynamic environment around radial sand ridges, the knowledge on the genesis of the radial tidal current is still in a very basic stage. This paper attempts to explore the influence of the tidal dynamics in large Shelf Sea on the formation mechanism of the local tidal current pattern using a schematized process-based model. Different incoming tidal signals are applied in this model respectively to investigate the related current pattern in RSRF. The results reveal that the radial current field only exists under some specified tidal signals from open sea. Furthermore, the geometry of the basin also plays a significant role in the formation of the current pattern.

**KEY WORDS:** Radial tidal current field, Radial sand ridges, Formation mechanism, Schematized model, Tidal wave.

## 1 INTRODUCTION

Linear sand bodies are often found in many geological settings where sufficient sediment is available and hydrodynamic process is strong (Off, 1963). In the central part of Jiangsu coastline, there exists a series of shore-face connected sand bodies taken Jianggang as the center (Figure 1). These sand bodies are known as radial sand ridges which cover an area of 22,470 $km^2$ and are made up of 70 sand ridges of different sizes (Wang, 2003). According to the field observations and numerical simulations, the pattern of the tidal current field is the same with the distribution of the radial sand ridges, which is: the tidal currents convergence and divergence in the radial sand ridge field during flood and ebb tide respectively. These unique radial sand ridges with radial tidal current have drawn many scientific attentions since 1950s. Many researches are conducted to improve the understanding on the formation, maintenance and evolution from both academic and practical interest (Ren et al., 1986).

Tide, specially, semi-diurnal tide, is thought to be one of the most important hydrodynamic processes in Jiangsu coast, while the effect of waves and other physical forcing are playing a subordinate secondary role (Wang, 2003; Liu and Xia, 2004). The tidal wave propagation pattern in the South Yellow

Sea has been well studied by numerical modeling (Yang, 1985; Zhu et al., 1995; Zhu and Yan, 1998; Zhang and Li, 1999; Zhu and Chang, 2001). And the tidal elevation amphidromic system in the South Yellow Sea is the main factor on both tidal elevation and tidal current pattern. Furthermore, on the formation of the radial current pattern off the central Jiangsu Coast, it is thought to be influenced by the meeting of two tidal wave systems—rotating tidal wave system in the South Yellow Sea and the incoming tidal wave from the East China Sea (Wang, 2003). Zhang et al. (1999) proposed a very classic theory on the dynamic mechanism of the RSRF area, which can be summarized as "Tidal current-induced formation--storm-induced change--tidal current-induced recovery". So, strong tidal currents are the main factor on the formation and the maintenance of the RSRF. Song et al. (1998) and Zhu and Chang (1997) successfully simulated the radial current pattern under the conditions of the flat seabed and a linear sloped topography using numerical modeling, respectively. Additionally, the simulation of Paleo-tidal current field in South Yellow Sea also proved that this special current pattern existed 7000 years ago and the pattern has been very stable since the Holocene transgression period (Zhu, 1998). Many numerical simulations have proved that the special tidal current pattern is not only independent of the local bathymetry, but also playing an crucial role in the formation of radial sand ridge system (Wang, 2003).

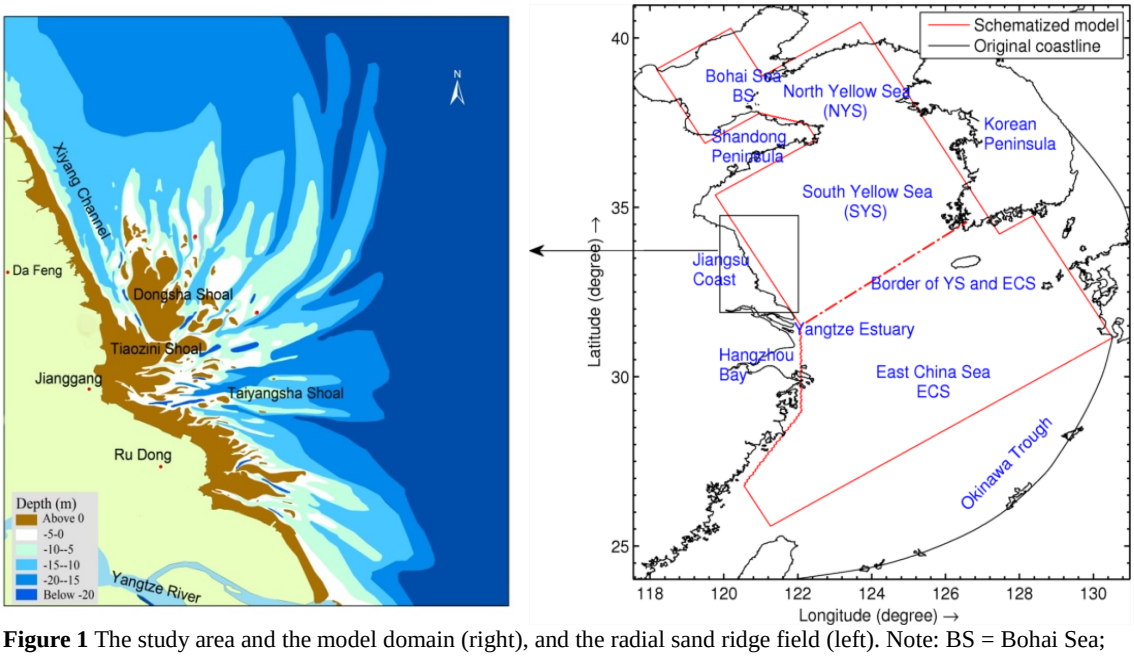


**Figure 1** The study area and the model domain (right), and the radial sand ridge field (left). Note: BS = Bohai Sea; NYS = North Yellow Sea; SYS = South Yellow Sea; ECS = East China Sea.

On the other hand, some idealized analytical models are proposed to obtain more deep insight into the tidal dynamics in such shallow water zones like the East China Sea, the North Sea etc. by extending the Taylor's solution (Taylor, 1922). Compared with the numerical solutions, the analytical solutions on the idealized basin are very helpful to distinguish the influence factors on the tidal dynamics. The classic analytical solution for tidal waves in a rectangular basin of uniform depth was first obtained by Taylor (1922). Taylor considered that the tidal wave in a semi-enclosed basin consisted of a linear superposition of incident and reflected Kelvin waves and an infinite number of Poincaré waves. Kang (1984) first used a rectangular basin with an opening at the head to represent the South Yellow Sea and investigated the asymmetry of the amphidromic system. He found that the asymmetry of amphidromic system aroused primarily due to a partial penetration of tidal energy through the opening at the bay head. Ye and Chen (1987) examined the effect of the seabed topography on tidal amphidromic system. He found that in the shallow water zones, the shift of the amphidromic points was mainly due to bottom friction; otherwise, the effect of the topography was the main factor. The study of Jung et al. (2005) also showed the variations in depth, bottom friction and the open heading in the boundary conditions all contributed to the determination of the formation of amphidromic points as well as overall patterns of $M_2$ tidal distribution.

With the help of the analytical method, the tidal dynamics and the corresponding influence factors can be well investigated. However, this method uses many unavoidable hypotheses and is only applied in the idealized condition.

Most numerical modeling focuses on the tide dynamics and the local morphological changes, whereas the analytical solutions concentrate on the tidal wave dynamics under different influencing factors. However, very little attention is paid to the tidal current systems and tidal current pattern in the South Yellow sea or the whole East China Sea. Since the tidal current and tidal elevation pattern are the two components of the propagation of the tidal wave, only focusing on tidal elevation amphidromic system to deduce the formation mechanism of the radial tidal current is not comprehensive. Therefore, we combine the method of the analytical solutions and the numerical modeling, in order to study the tidal current systems in the whole East China Sea, and the formation mechanism of the radial pattern of the tidal current through analyzing the different influence factors. In this study, we first develop a schematized process-based model to analyze the tidal dynamics with the consideration of the analytical method. Several experiments are carried out to test the sensitivity of the tidal currents under different conditions.

## 2 MODEL SETUP AND PERFERMENCE

In the former analytical solutions of the tidal dynamic pattern in the South Yellow Sea, the domain is often simplified to be a regular tidal basin with uniform or linear water depth. In our numerical modeling, we take advantage of the method used in analytical models, and first simplify the domain of the Chinese marginal sea to be a regular basin, but using more actual bathymetry. The schematized 2D model is developed based on Delft3D modeling system. Delft3D fully integrates the effects of waves, tide and sediment with on line morphological update in coastal, river and estuarine regions (Lesser et al., 2004). Here, we only consider the tide neglecting the waves and sediment, because the scale of the study area is relative large and our aim is focusing more on the tidal current pattern.

### 2.1 Model domain and boundary conditions

The schematized model domain covers the area of the whole Chinese marginal seas (Figure 1). It should be noted that, the purpose of the schematized model is not to simulate the tides in the Chinese Marginal Sea accurately, but to examine the general features of the tidal elevation and tidal current pattern and to find the deep reason causing the special tidal current in the central Jiangsu coast. So, we made some simplifications on the studying area. The irregular coastlines are changed to be straight lines but following the trend of the coast and keeping the main features. Through this simplification, the general shape of most of the Chinese coastline is conserved, for example, the shape of Shandong Peninsula, Yangtze River Estuary etc., and neglect the influence of the (local) irregular coastline shape. In addition, the Bohai Sea has been idealized as a rectangular basin, and this simplification has little influence on the tidal wave pattern in the South Yellow Sea, because the incoming tidal energy to the Bohai Sea from the Yellow Sea only account for 6.86% of that into the Yellow Sea from the East China Sea (Fang, 1979).

The model used the rectangular grid with a grid size of 3’×3’ approximately, under the spherical coordinate. The bathymetry of the model is generated by Delft3D-QUICKIN Module according to the actual seabed topography (Figure 2). Open boundary conditions are prescribed by a large-scale China Sea model. 8 main tidal constituents are specified along the open boundary of the schematized model as the drive forcing for the water motion.

### 2.2 Model results and analysis

The simulation period of the model is set to one month with a time step of 3 minutes considering for a stable and accurate computation (Courant number < 10). Online Fourier analysis is carried out in every grid point of the domain, so it is easy to get the information of the tidal wave pattern through analysis of the tidal elevation and tidal current. Since the semi-diurnal tides are the dominant components in the domain, here we only focus on the feature of the $M_2$ constituent. Tidal elevation pattern is shown by co-tidal chart of the $M_2$ constituent in the whole domain (Figure 3). The tidal elevation amphidromic points (EAP) in the Yellow Sea which have a significant influence on the local tidal pattern is well simulated by the schematized model. Also, in the central Jiangsu Coast and RSRF area, the amplitude is

increased greatly, forming a region with large amplitude about 1.8m. This feature is similar to the actual tidal characteristics of RSRF area (Chen et al., 1992).

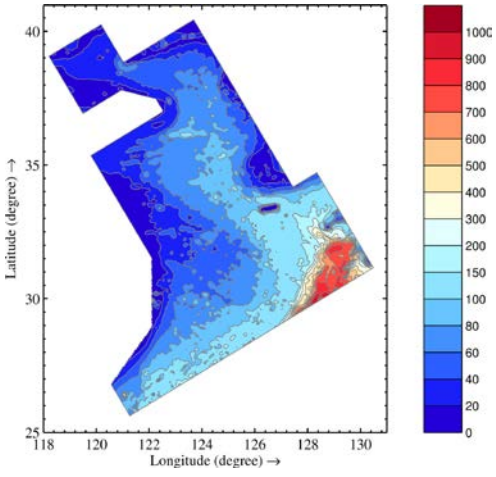


**Figure 2** Bathymetry of the Schematized model.

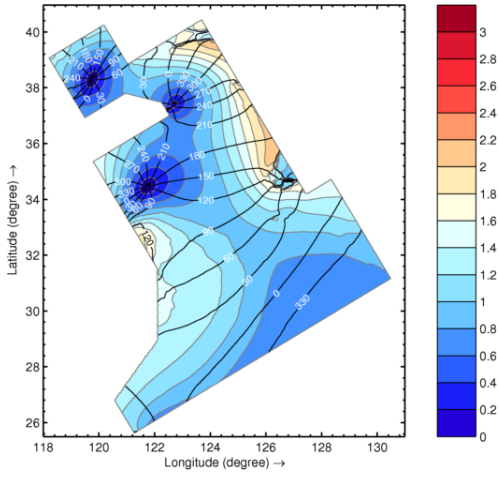


**Figure 3** Co-tidal chart of $M_2$ constituent (tidal elevation).

Tidal current patterns are shown in Figures 4 to 7. The tidal ellipse field (Figure 4) displays that the tidal currents show a great potential moving convergent and divergent towards one center (focal point of the radial current, referred to FP in the following of this paper), which is the city of Jianggang in reality. In the north of Jiangsu coast (area A in Figure 4), the tidal current are mostly the reciprocating flows. However, outside the Yangtze River Estuary and south of radial sand ridges (area C and B in Figure 4, respectively), the tidal current ellipse type is rotary. Same phenomena can be found from the distribution of the tidal current ellipticity in the basin (Figure 5). Along the northern Jiangsu Coast, the ellipticity is about 0.2, and in the southern RSRF (area B in Figure 5) and the area off the Yangtze River Estuary (area C in Figure 5), the ellipticity is from 0.6 to 0.8, showing a sense of rotation. Besides, in the middle of the South Yellow Sea, there is a zero ellipticity line crossing through the whole area, and the South Yellow Sea is divided into two sections. In the north part the tidal currents flow in the anti-clockwise direction, while the south part is moving clock-wisely.

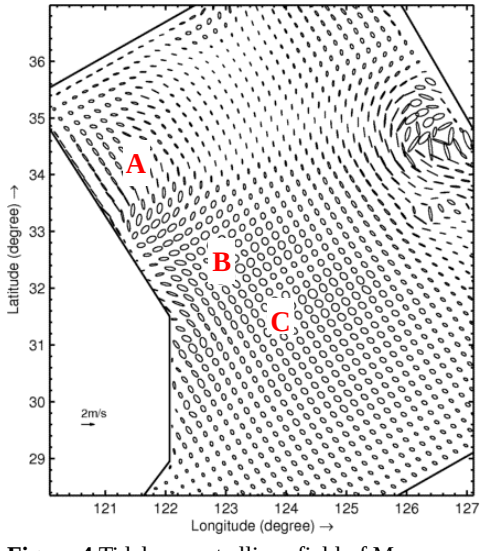


**Figure 4** Tidal current ellipse field of $M_2$ constituent (enlarged in South Yellow Sea).

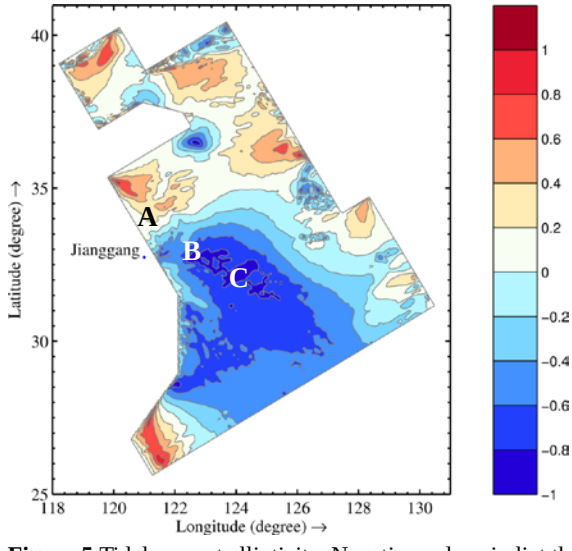


**Figure 5** Tidal current ellipticity. Negative values indict the rotation is clockwise; positive values show the anti-clockwise rotation

Figure 6 and 7 are the co-tidal current charts of $M_2$ constituent. Compared with the co-tidal charts of the tidal elevation, the shape of the current charts has considerable deformity and irregularity, but the main characteristics can still be recognized. It is clear that in the central Jiangsu Coast, the magnitude of the tidal current velocity is strong and in the center of the South Yellow Sea, there exists a zone of the weak tidal current (Figure 6). Two current amphidromic points (CAPs) can be found near the south Shandong Peninsula: one is located in the head of the Shandong Peninsula and center of the Yellow Sea, and the other is in the southwest corner of the South Yellow Sea corresponding to the Haizhou Bay in reality (Figure 7). In fact, according to the study of Xia et al. (1995), the CAPs are closely connected to the EAPS in a basin and often found between two EAPs. So, the CAPs in the South Yellow Sea indeed in the area between the two EAPs in North Yellow Sea and South Yellow Sea (Figure 3). The CAPs is often related to the areas of weak flow, but the velocity is not necessarily zero just with a large ellipticity (for example, the ellipticity equal to 1), which is different from the characteristics of the EAP. Meanwhile, the position of the two CAPs is consistent with the large ellipticity zone near the south Shandong Peninsula shown in Figure 5. It is indicated that our schematized model could simulate the basic pattern of the tidal flow.

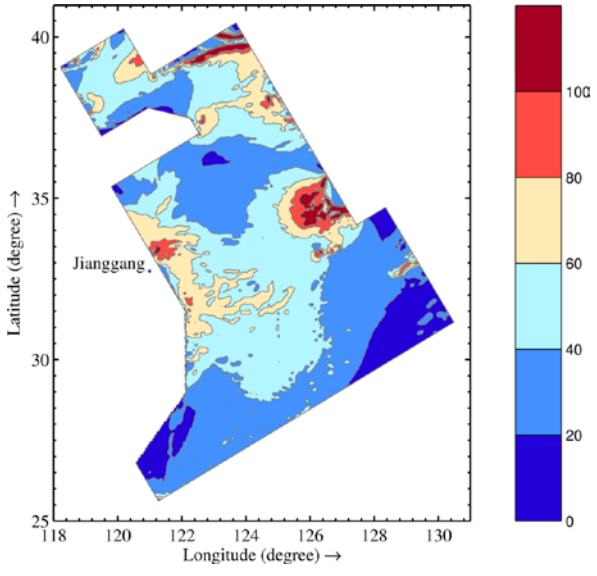


**Figure 6** Co-amplitude chart of the $M_2$ tidal current*.

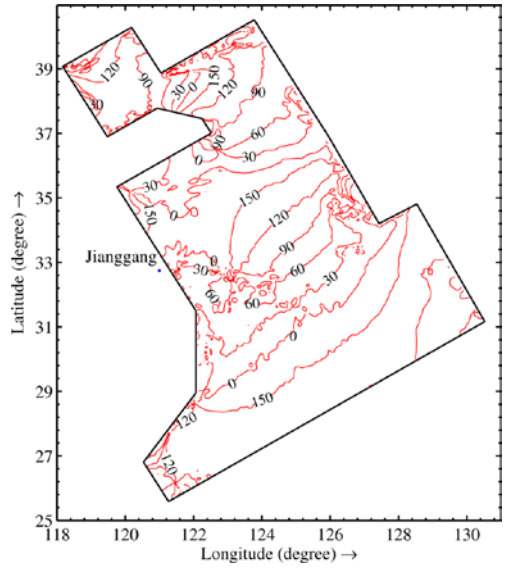


**Figure 7** Co-phase lines of the $M_2$ tidal current∞.

In addition, in order to assess the schematized model, we compared the results with previous literatures and observations (Table 1). Here we only listed the position of the AP and FP of the current field off the central Jiangsu Coast. Table 1 shows that the amphidromic system as well as the tidal current field simulated by the schematized model have slightly differences from both the results of previous tidal wave models using real geometry and the observation. The difference is mainly due to the deviation between different calculation methods. So, our model has a good agreement with the previous results in the RSRF and South Yellow Sea, and has the capacity to conduct numerical experiments. Besides, the good agreements also show that the resolution of the coastline has less effect on the tidal dynamics, because even under the condition of the regular coastline shape, the tidal dynamics is still hardly changed.

* Co-amplitude lines of the tidal current are the lines of the equal semi major axis (maximum velocity of the tidal current) of the tidal current ellipse. Note: the unit of the velocity is cm/s.

∞ Co-phase lines of the tidal current are the lines of the equal phase (time) when the tidal current reach to the maximum velocity. Note: the unit is degree, ranging from 0° to 180°.

**Table 1** Comparison between the results and the previous studies.

| Models | Position of AP | Position of the FP |
|---|---|---|
| Schematized model (this paper) | 121°45′E, 34°27′N | 121°30′E, 32°30′N |
| Marine Atlas (Chen et al., 1992) (Observation) | 121°33′E, 34°15′N | 121°12′E, 32°29′N |
| Fang (1986) (Chinese sea model) | 121°40′E, 34°40′N | -- |
| Zhang (2005) (Chinese Sea model) | 121°26′E, 34°34′N | 121°06′E, 32°50′N |
| Xing (2011) (South Yellow Sea model) | 121°38′E, 34°38′N | 121°00′E, 32°41′N |

## 3 SENSITIVITY EXPERIMENT RESULTS AND DISCUSSION

In the real ocean, the different shape of the basin, different incoming tidal waves, complicated bathymetry, bottom friction and irregular shoreline etc. have important influences on the sea surface elevation and even greater impacts on the tidal current. In order to get a more clear knowledge about tidal wave propagate pattern and further the tidal current pattern along the Jiangsu coast, a series of experiments based on this schematized model are designed and conducted. Here we focus on the different incoming tidal energy on this special tidal basin with specified boundary shape aimed to find the deep reason influencing the tidal current pattern along the Jiangsu Coast. Different tidal signals are applied along the open boundaries to test the response of the tidal current and to analyze under which condition there will exist the tidal current field, as well as the main reason caused the special current pattern in the central Jiangsu Coast.

### 3.1 Sensitivity experiment settings

It is well known that the semi-diurnal tides (especially $M_2$ constituent) are the main tidal type in the South Yellow Sea. But it is still not clear what will happen if a different single constituent at the open boundary with the same amplitude and phase as the $M_2$ constituent but different frequency is prescribed. In other words, if the local tide is not a semi-diurnal tide but a diurnal tide, 1/3 diurnal etc., it is not clear whether the radial tidal current will continue to exist or not. In this part, the influence of tide constituent frequency on the radial tidal current is analyzed through a series of experiments. These experiments use the same phase-lag and amplitude as the $M_2$ constituent but different period (or different frequency) as boundary conditions, to represent different incoming tidal waves.

For simplification, we assume that there is only one tidal constituent at open boundary to prescribe the tidal motion. So, in each experiment, we set one tidal signal with specific period along the open boundary. And the amplitudes and phase-lags in these points of the open boundary are the same as the $M_2$ constituent, which has been used in the original schematized model. During numerical experiment, a total of 41 groups of experiments are conducted covering the tidal wave period from 24h to 4h with an interval of 0.5h. Because the shape of the basin is pre-determined and the bathymetry is generated based on the real topography, changing the frequencies of the incident tidal wave will generate different wave length of the tidal wave in each case. In each simulation, we record the tidal elevation and tidal current information in order to have a full view of the effect of different incident tidal wave and establish the relationship between the different tidal wave and the response of the tidal current field.

### 3.2 Results and discussion

#### 3.2.1 Focal point (FP) response to different incident tidal wave signals

The existence of the radial tidal current field and the focal point of the current field are recorded in each experiment according to the simulation result. Based on this, the relationship curve between the incident tidal wave and the radial current field is drawn (Figure 8). For convenience, we use the frequency of tidal cycles per day to represent different incoming tidal waves. The position of the radial tidal current is identified by the distance between the FP and the Shandong Peninsula. From Figure 8, we discover that if the frequency of the tidal cycle per day is small, there is no radial current field in the central Jiangsu Coast. Same phenomena can be found with high frequencies of the tide. The radial current field firstly appears in the breakpoint B, corresponding to the wave period of 14.5h. But the position of this radial tidal current field is near the area of Yangtze Estuary not the central Jiangsu Coast, and the range of the current field is small according to Figure 10(B). With the increase of the frequency of the tidal cycle, the

position of the tidal current field become stable and is finally stopped in the central Jiangsu Coast. So, it can be concluded that the existence of the radial current field only can be found in such specified range of the tidal frequency (that is: from 2 to 2.8 tidal cycles per day). And if the tidal frequency is less than 1.5 times per day or more than 3.2 times per day, there is no radial current field. That is to say, no clear radiation distribution of the current field can be found on the condition of either large or small frequency tidal waves. Only in the range of 2 to 2.8 (the period of incident tidal wave is from 8.5 to 12 hour), there will form the large area stable tidal current field with radial distribution and take the city of Jianggang as a center. The real tide in central Jiangsu Coast is the typical regular semi-diurnal tide with the period of 12.4h which is slightly beyond the limit of the range as shown in Figure 8, but the radial tidal current field is still existed (Figure 4). The difference is focusing on the magnitude of the tidal current velocity and the power of the convergent and divergent flow. In summary, the relationship curve indicates that the tidal components between the semi-diurnal and a one third diurnal tides can influence the existence of the radial tidal current field in central Jiangsu Coast under this specific water depth and land boundary shape.

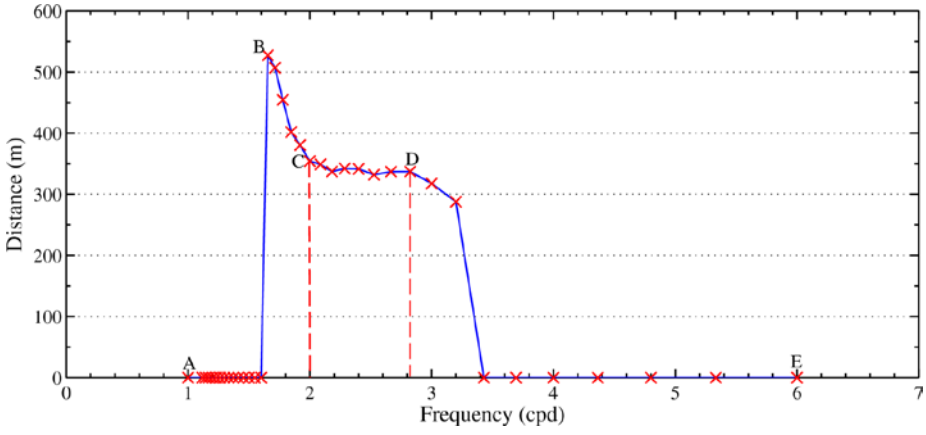


**Figure 8** Relationship curve between the radial tidal current and the incident tidal wave. Note: The distance indicates the distance between the FP and the south boundary of the Shandong Peninsula. Zero dots represent the absence of the radial tidal current field

### 3.2.2 Movement of the tidal elevation amphidromic points (EAPs)

In each experiment, we also obtained the tidal elevation co-tidal charts based on simulation results. The movement of the tidal elevation amphidromic points (EAPs) under the change of incident tidal waves is captured and shown in Figure 9. In order to facilitate the comparison, we also marked letters from A to D corresponding to Figure 8. It can be seen that, in the case of low frequency of the incoming tidal wave, there is only one EAP in the Yellow Sea with its position shifting from the center axis. Under this condition, the wave length is relatively large and it is less sensitive to the irregular end of the basin (the boundary of the Shandong Peninsular and the North Yellow Sea).

With the increase of the frequency of the tidal cycles, the EAP begins moving towards north and then disappeared or hiding inside of the Shandong Peninsula (Figure 9). It implies that the reflected tidal wave will meet the incoming tidal wave in the position of the Shandong Peninsula forming the amphydromic system close to the boundary side. Besides, it also indicates the reflected tidal wave caused by the Shandong Peninsula is less than the North Yellow Sea part, because if the effect of the Peninsula is large, the amphidromic system will never be close to its boundary and the amplitude near the boundary will be large.

The second EAP will appear if the frequency keeps growing as the red stars shown in Figure 9. From this point, the effect of the Shandong Peninsula become more and more important on the amphidromic system in the South Yellow Sea, whereas the influence of the reflect tidal wave from the North Yellow Sea gradually limited in the local area. The tidal wave system separates into two relatively independent amphidromic systems. So, the irregular boundary shape in the end of the basin begin to show significant influence on the tidal wave. Based on the results of different experiments, it can be found that the distance

between the south boundary of the Shandong Peninsula and the north boundary of the North Yellow Sea is the control factor for the separation of the tidal wave in the Yellow Sea, if ignoring the tidal energy dissipating into the Bohai Sea. Furthermore, as this distance is fixed, while the tidal wave length is a variable in the experiments, it can be indicated that the ratio $\beta$ between these two lengths is the important factor influencing the tidal wave system in the Yellow Sea. That is:

$$\beta = \frac{D_{SN}}{\lambda_{in}} \tag{1}$$

in which $D_{SN}$ is the vertical distance between the south boundary of the Shandong Peninsula and the north boundary of the North Yellow Sea, in this schematized model $D_{SN}$ is fixed value, which is equal to 245 km, approximately; $\lambda_{in}$ is the incident tidal wave length, which depend on the incoming tidal wave applied to the open boundary. So, in this case which the tidal wave period is 16.5h, the wave length can be calculated according to the water depth and wave period in the basin, which is 1250km, approximately, so the ratio $\beta$ is about 0.2, equivalent to 1/5 wavelength. That is to say, if the incoming tidal wave length decreased to the 5 times as much as the $D_{SN}$, the irregular boundary shape in the end of the basin become important on the propagation of the tidal wave. It should be noted that this proposed ratio $\beta$ is just to give a qualitative idea of when the irregular boundary will influence the tidal wave system and provide a preliminary judgment.

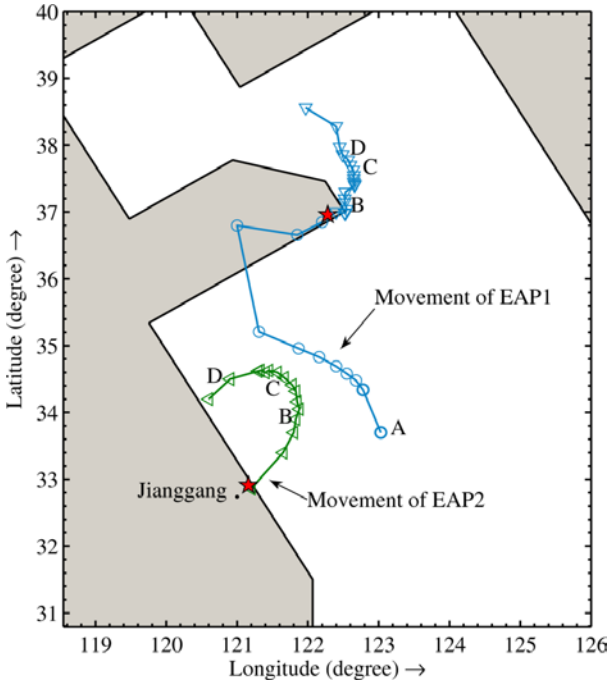


**Figure 9** Movement curves of the tidal elevation amphidromic point (EAP) during different incoming tidal waves. Note: here, the first appeared EAP in the Yellow Sea is named EAP1, marked with blue lines and circles, and after the second EAP (EAP2) appeared, the EAP1 is labeled by the blue triangles. The EAP2 is shown by the green triangles. Letters (from A to D) are corresponding to the breakpoint in Figure 8.

When the EAP2 reach the breakpoint C, the EAP2 moves to the coast and the trace is parallel with the Shandong Peninsula. So, that is why there will exist a stable radial tidal current field in the central Jiangsu Coast (Figure 8) between the specific tidal period. From point C to D, the ratio $\beta$ is change from 0.27 to 0.4. In other words, both the EAP2 and the current field are stable when the incoming tidal wave length is between the 2.5 and 3.7 times as much as the $D_{SN}$. And for the Jiangsu Coast where the $M_2$ tidal constituent dominates, the ratio $\beta$ is about 0.26 with the tidal period of 12.42 hour. On one hand, this value is close the range we obtained. On the other hand, it also implies that the radial tidal current field in the central Jiangsu Coast is not at its best conditions.

According to the simulation, if the tidal frequency is larger than 3.5 cycles per day, the tidal wave system become very complicated with more than one tidal amphidromic systems in the South Yellow Sea. And it is not necessary to consider this condition, because this kind of tidal wave with large frequency is mainly found in the small local region caused by the boundary effect, increased non-linear bottom friction in the shallow water zone.

### 3.2.3 The response of the tidal current systems

Figure 10(A) is the tidal ellipse field and the magnitude of the ellipticity in case of the one tidal cycle per day. It can be seen that the tidal flow is very weak in the basin when the wave length is large. The tidal currents become stronger with the decrease of the wave length shown in Figure 10(B). The frequency is about 1.65 tidal cycles per day, and the ellipticity in the south of Jianggang and outside the Yangtze Estuary is small, about 0.2. Combined with the ellipse field, it can be found that the radial current begins to appear, but the FA is located near the Yangtze Estuary rather than the city of Jianggang. The distribution of the ellipticity also shows that the clockwise flow is account for a large area of the South Yellow Sea, while the anti-clockwise current area is relatively small. It is indicated that the amphidromic system in the South Yellow Sea is still weak and not well developed.

Figure 10(C) and 10(D) show the cases with the stable current field with the frequency of 2 and 2.8 respectively. In these two cases, it can be seen that the FP of the current field mainly stay in the city of Jianggang but the magnitude of the current in Figure 10(D) is larger than in the 10(C). In other words, the tidal flow is enhanced considerably when the wave frequency turned to be high. Besides, it also implies that the amphidromic system in the South Yellow Sea is well developed and become the dominate factor for the water motion. There are two parts with the opposite flow direction in the South Yellow Sea according to Figure 10(C), whereas the current with the clock wised rotation occupies almost the whole region in Figure 10(D). This phenomena is consistent with the landward motion of the EAP2 in the South Yellow Sea (Figure 9). That is because the anti-clockwise flow in the north part of the South Yellow Sea is mainly controlled by the amphidromic system (which is also the anti-clockwise direction in the northern hemisphere), and when the EAP2 move to the landward, the area influenced by the amphydromic system become smaller and finally limited in the near shore zone. However, even under this condition, the trend of the radial current field is still obvious as well as the strong tidal flow. So, the lateral movement of the EAP2 influences little on the existence of the radial current field but indeed influence the magnitude of the flow and distribution of the tidal ellipse.

If the tidal wave frequency keep increasing, the tidal current will be influenced greatly by the local bathymetry, bottom friction etc. and become more complicated. Meanwhile, the radial current field will disappear with the further increase of the frequency of the tidal cycles.

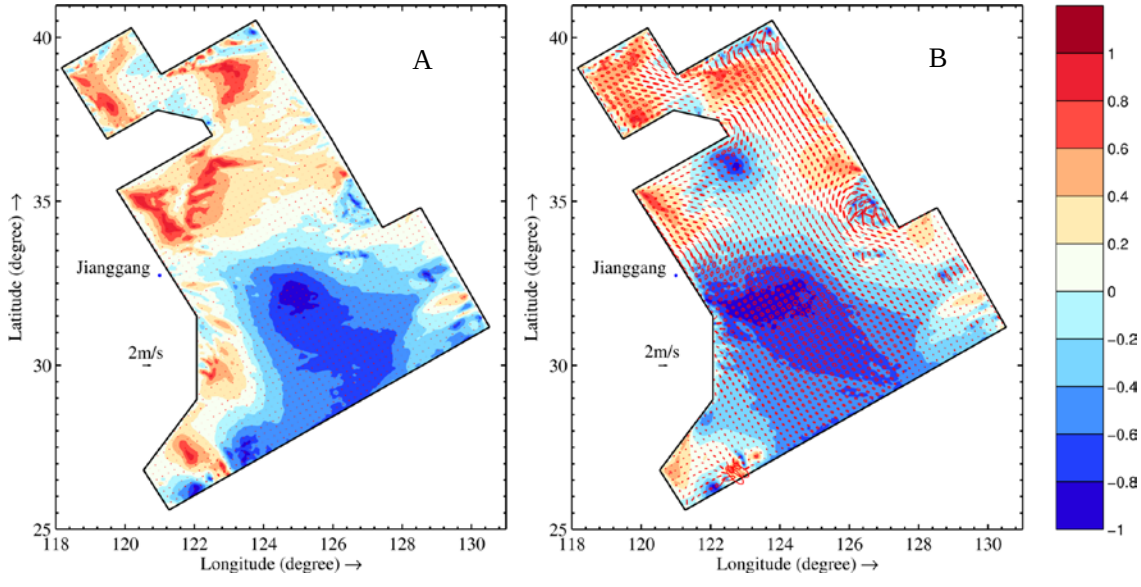

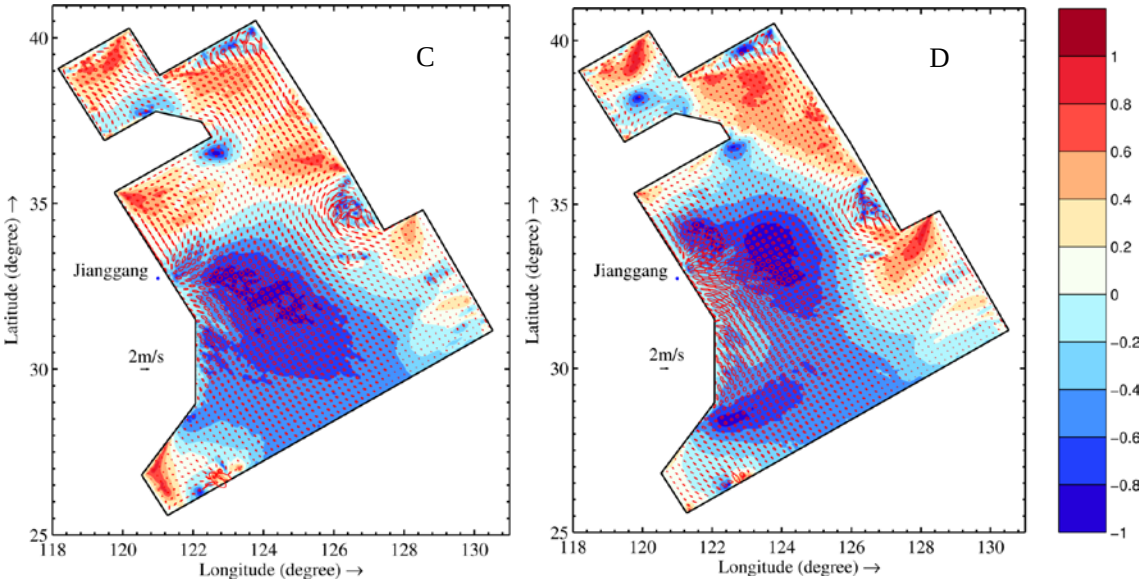


**Figure 10** Tidal ellipse field and ellipticity distribution in the basin. Note: The background maps are the ellipticity distribution; the negative values indict the rotation is clockwise; positive values show the anti-clockwise rotation. Letters (from A to D) are corresponding to the breakpoint in Figure 8.

## 4 CONCLUSION

In this paper, the process-based schematized model is developed to investigate the deep reason for the formation of the radial tidal current field in the central Jiangsu Coast. The method for the influence factors analysis is with reference to the analytical models on tidal wave. The combination of the numerical and analytical model can provide more detailed analysis about the tidal dynamic mechanism on the whole Chinese marginal sea. Different incident tidal waves are defined along the open boundaries of the basin to investigate the response of the local tidal current field and to explore the relationship between incident tidal wave and radial tidal current off the central Jiangsu Coast. The conclusions are as follows:

Firstly, the results suggest that under specified depth and basin geometry, the incoming tidal waves indeed influence the existence of the radial tidal current off the central Jiangsu Coast. And based on our experiments, the radial tidal current only appears in such specific tidal constituents between the semi-diurnal and a one third diurnal tides.

Secondly, in this specific basin, our experiments show that the relation between the end boundary shape and incoming tidal wave is a fundamental factor in determine the position of the EAP in the Yellow Sea as well as the existence of the radial tidal current field. If the ratio $\beta$ is between 0.24 and 0.4, there will be two stable EAPs in the North Yellow Sea and the South Yellow Sea, respectively, and the tidal current field is the radial pattern.

Finally, even though the tidal current field is controlled by the amphidromic system in the South Yellow Sea, in a certain range of the incoming tidal frequency (for example, from 2 to 2.8 tidal cycles per day), the EAP moved landward gradually, while the position of the radial tidal current was stable with no change. But both the radial shape and the magnitude of the radial tidal current will be enhanced with the decrease of the tidal wave length.

## ACKNOWLEDGEMENT

The first author is financially supported by the China Scholarship Council. This study was additionally supported by the 111 Project of the Ministry of Education and the State Administration of Foreign Experts Affairs, China (Grant No. B12032).

**References**

Chen D., Sun X., Pu Y., 1992. Marine Atlas of Bohai Sea, Yellow Sea and East China Sea (Hydrology). China Ocean Press, Beijing (in Chinese).

Fang G., 1979. Dissipation.of tidal energy in Yellow Sea. Oceanologia Et Limnologia Sinica, 10, 200-213 (in Chinese).

Jung, K.T., Park, C.W., Oh, I.S., So, J.K., 2005. An analytical model with three sub-regions for $M_2$ tide in the Yellow sea and the East China Sea. Ocean Science Journal, 40(4), 191-200.
Kang, Y.Q., 1984. An analytic model of tidal waves in the Yellow Sea. Journal of Marine Research, 42(3), 473-485.
Lesser, G.R., Roelvink, J.A., van Kester, J.A.T.M., Stelling, G.S., 2004. Development and validation of a three-dimensional morphological model. Coastal Engineering, 51(8-9), 883-915.
Liu, Z., Xia, D., 2004. Tidal sands in China seas. Ocean Press, Beijing (in Chinese).
Off, T., 1963. Rhythmic linear sand bodies caused by tidal currents. Assoc. Petroleum Geologists Bull, 47(2), 324-341.
Ren, M., Xu, Y., Zhu, J., 1986. Comprehensive Investigation of the Coastal Zone and Tidal Land Resources of Jiangsu Province. Ocean Press, Beijing (in Chinese).
Song, Z., Yan, Y., Xue, H., Mao, L., 1998. Hydromechanics for formation and development of radial sandbanks-II vertical characteristics of tidal flow. Science in China (Series D), 28(5), 411-417(in Chinese).
Taylor, G.I., 1922. Tidal oscillations in gulfs and rectangular basins. Proceedings of the London Mathematical society, 2(1), 148-181.
Wang, Y., 2003. Radiative Sandy Ridge Field on Continental Shelf of the Yellow Sea. China Environmental Science Press, Beijing (in Chinese).
Xia, Z., Carbajal, N., Südermann, J., 1995. Tidal current amphidromic system in semi-enclosed basins. Continental Shelf Research, 15(2), 219–240.
Yang, Z., 1985. Sedimentology and Environment in South Huanghai Sea Shelf Since Late Pleistocene. Marine Geology & Quaternary Geology, 5(4), 1-19 (in Chinese).
Ye A., Chen Z., 1987. Effect of bottom topography on tidal amphydromic system in semi-enclosed rectangular waters. Journal of Shandong College of Oceanology, 17, 1-7 (in Chinese).
Zhang, C., Zhang, D., Zhang, J., Wang, Z., 1999. Tidal current-induced formation—storm-induced change—tidal current-induced recovery. Science in China Series D: Earth Sciences, 42, 1-12.
Zhang, J., Li, C., 1999. Producing Condition and Evolving Progress of the Tidal Sand Bodies in the Northern Jiangsu and the Southern Huanghai Sea. Acta Oceanologica Sinica, 21(2), 65-74 (in Chinese).
Zhu, Y., 1998. Numerical Simulation of Paleo-tidal Current Field in the Subei Littoral Plain Area and Its Verification. Marine Science Bulletin, 17(3), 1-7 (in Chinese).
Zhu, Y., Chang, R., 1997. Explanation of the Origin of Radial Sand Ridges in the Southern Yellow Sea with Numerical Simulation Results of Tidal Currents. Journal of Ocean University of Qingdao, 27(2), 218-224 (in Chinese).
Zhu, Y., Chang, R., 2001. Sediment Dynamics Study on the Origin of the Radial Sand Ridges in the Southern Yellow Sea. Studia Marina Sinica, 43, 38-50 (in Chinese).
Zhu, Y., Li, C., Chang, R., 1995. Numerical Explanations on Genesis of the Jianggang Radial Sandbanks with Relevance of Ancient Eviroment. Journal of Tongji University, 23(Suppl.), 226-230 (in Chinese).
Zhu, Y., Yan, Y., 1998. Tidal Current Numerical Model for the Formation and Development of Radial Sandbank in the Yellow Sea. Journal of Hydrodynamics: A Series, 13(4), 473-480 (in Chinese).